A ternary cascade structure enhances the efficiency of polymer solar cells†

Jen-Hsien Huang,[a] Marappan Velusamy,[b] Kuo-Chuan Ho,[cd] Jiann-Tsuen Lin*[b] and Chih-Wei Chu*[ae]

Received 7th September 2009, Accepted 7th January 2010
First published as an Advance Article on the web 15th February 2010
DOI: 10.1039/b918362k

In this study, a novel solution-processed small molecule (TQTFA) for use as an electron donor has been incorporated into organic solar cells based on poly(3-hexylthiophene) (P3HT) and (6,6)-phenyl C71-butyric acid methyl (PC[70]BM). The combination of TQTFA with P3HT and PC[70]BM allows not only a broad absorption but also tuning of the inter energy level leading to a higher short-circuit current (J_{SC}) and open-circuit voltage (V_{OC}). The best performing devices exhibited a power conversion efficiency of 4.50%. The efficiency is increased by almost 15% when compared to the one without TQTFA.

1. Introduction

Photovoltaic technologies continue apace towards the goal of renewable solar energy, which promises to eliminate the energy crisis and protect the environment. Among the thin film photovoltaic technologies, the study of organic solar cells (OSCs) is a promising route towards realizing large-area, flexible devices providing low-cost energy.[1,2] Because of their ultra fast rates of charge transfer and large donor–acceptor interfaces for exciton dissociation,[3,4] polymer/fullerene bulk heterojunction (BHJ) solar cells have been studied most extensively to boost the efficiency of polymer solar cells.[5–7] Controlling the donor and acceptor morphologies in BHJ solar cells incorporating poly(3-hexylthiophene) (P3HT) as a donor and [6,6]-phenyl-C_{61}-butyric acid methyl ester (PCBM or PC[60]BM) blend as an acceptor has led to maximum external quantum efficiencies (EQEs) of *ca.* 70% and power conversion efficiencies (PCEs) of 4–5%.[8–11] Although great process developments have improved, the charge transfer properties of P3HT/PCBM-based solar cells, the large band gap of P3HT and the large offsets of the energy levels of the highest occupied molecular orbitals (HOMOs) and the lowest unoccupied molecular orbital (LUMOs) of P3HT and PCBM means that there are limitations of high performance and commercialization of these devices.[12,13] Hence, to further improve the efficiency of polymer solar cells, it is likely that research efforts will continue to focus on synthesizing new donors and acceptors and developing innovative architectures.

Recently, the energy harvesting capabilities of OSCs have been improved through the use of low band gap conjugated polymers.[14–20] Although the absorption spectra of these polymers extend into the long wavelength regime (*e.g.*, near-infrared), they still sacrifice some absorption in the visible region. Moreover, the offsets of the HOMO energy levels of the donors and acceptors lead to significant energy losses upon exciton dissociation. Therefore, to enhance photocurrent generation, there remains great interest in combining organic semiconductors that exhibit complementary spectra. For example, the use of cascade multilayer device structures in solar cells can enhance the device performance.[21–23] Nevertheless, most of these multilayer devices have been fabricated using complicated and time-consuming thermal evaporation processes. A common strategy for forming thin films from two or more dissimilar soluble materials is to mix them together. This approach is used extensively in the preparation of polymer light-emitting diodes,[24,25] but it has not been quite as successful in the fabrication of polymer solar cells.[26,27] When attempting to prepare efficient BHJ solar cells incorporating three blended organic semiconductors, three criteria must be considered for the third organic semiconductor: (i) its energy levels must have the correct offset with respect to those of its blend counterparts; (ii) it can operate as either an electron acceptor and transport or an electron donor and hole transport; and (iii) it should have high absorption coefficients in complementary absorption ranges with respect to those of its blend counterparts.

In this study, we used the newly developed conjugated small molecule 7,7′-{5,5′-[10,12-bis(4-*tert*-butylphenyl)dibenzo[*f*,*h*]thieno[3,4-*b*]quinoxaline-2,7-diyl]bis(thiophene-5,2-diyl)}bis(9,9-dihexyl-*N*,*N*-diphenyl-9*H*-fluoren-2-amine) (TQTFA, Fig. 1(a))[28] to form a ternary cascade structure in BHJ solar cells. Photoluminescence (PL) quenching measurements confirmed that charge transfer occurred between P3HT and TQTFA and between TQTFA and PCBM. Moreover, TQTFA acts as an electron acceptor and electron donor in combination with P3HT and PCBM, respectively. Cascade BHJ solar cells having the structure P3HT/TQTFA/[6,6]-phenyl-C_{71}-butyric acid methyl ester (PC[70]BM) exhibit enhanced photocurrent densities and open circuit voltages relative to those of solar

[a]*Research Center for Applied Sciences, Academia Sinica, Taipei, Taiwan 11529. E-mail: gchu@gate.sinica.edu.tw*
[b]*Institute of Chemistry, Academia Sinica, Taipei, Taiwan 11529. E-mail: jtlin@chem.sinica.edu.tw*
[c]*Department of Chemical Engineering, National Taiwan University, Taipei, Taiwan 106*
[d]*Institute of Polymer Science and Engineering, National Taiwan University, Taipei, Taiwan 106*
[e]*Department of Photonics, National Chao-Tung University, Hsinchu, 30010, Taiwan*
† Electronic supplementary information (ESI) available: Experimental data. See DOI: 10.1039/b918362k

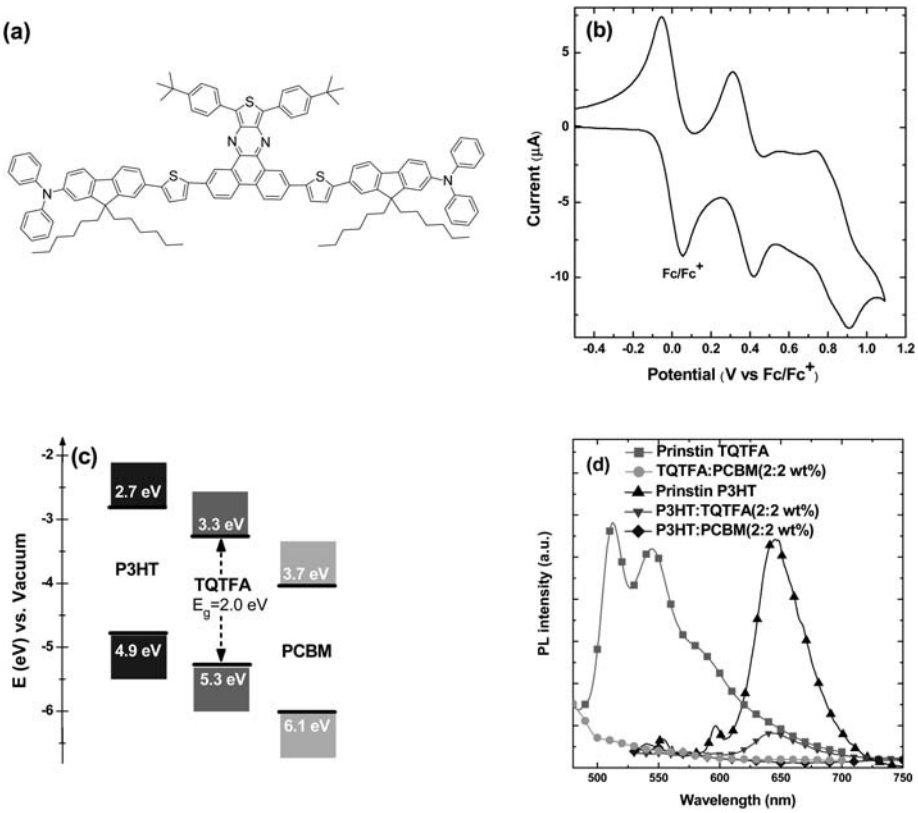

Fig. 1 (a) The chemical structure of TQTFA. (b) Cyclic voltammogram of a TQTFA film cast on a Pt wire, measured in 0.1 M $(n\text{-}C_4H_9)_4NPF_6/CH_2Cl_2$ at 50 mV s^{-1}; potentials are quoted with reference to the internal ferrocene standard ($E_{1/2}$ = +212 mV *vs.* $Ag/AgNO_3$). (c) Energy level diagram for P3HT, TQTFA, and PCBM. (d) PL spectra of pristine P3HT and TQTFA in the solid state and PL quenching for P3HT:TQTFA, P3HT:PCBM, and TQTFA:PCBM blends.

cells featuring P3HT/PC[70]BM as the active layer, presumably because of the appropriate light harvesting and energy levels of TQTFA.

2. Experimental

Materials

The TQTFA was synthesized according to the reported procedure.[28] The P3HT was purchased from Rieke Metals. The regioregularity, weight (*M*w), number (*M*n) average molecular weights, and polydispersity index (PDI) of RR-P3HT are as follows: regioregularity = 93%, *M*w = 3.7 × 10^4, *M*n = 2.5 × 10^4, and PDI = 1.48, respectively. The PCBM was purchased from Nano-C.

Device fabrication

The polymer photovoltaic devices were fabricated by spin-coating (3000 rpm, 60 s) blends of P3HT, TQTFA, and PCBM (at certain weight ratios in DCB) onto a poly(3,4-ethylenedioxythiophene):poly(styrenesulfonate) (PEDOT:PSS)-modified ITO surface. Next, 30 and 100 nm thick layers of Ca and Al, respectively, were thermally evaporated under vacuum at pressures of less than 6 × 10^{-6} torr.

Characterization

The cell performance was tested under simulated AM 1.5 G irradiation at 100 mW cm^{-2} using a Xe lamp-based solar simulator (Thermal Oriel 1000 W). The light intensity was calibrated using a mono-silicon photodiode equipped with a Hamamatsu KG-5 color filter. The whole measurement process was performed at room temperature in a glove box filled with N_2. Cyclic voltammogram (CV) studies were performed with a three-electrode cell with 0.1 M $(n\text{-}C_4H_9)_4NPF_6/CH_2Cl_2$ and a Pt wire as the working electrode, a Pt sheet as the counter electrode, and non-aqueous Ag/Ag^+ (containing 0.01 M $AgNO_3$ and 0.1 M TBA-ClO_4 in MeCN) as the reference electrode. To measure the absorption and PL emission properties of the polymer films, samples were fabricated on a glass substrate. The UV-Vis absorption spectra were measured using a Jasco-V-670 UV-Vis spectrophotometer. PL spectra were obtained using a Hitachi F-4500 photoluminescence spectrometer. Surface morphologies were observed through AFM using a Digital Instrument NS 3a controller equipped with a D3100 stage. The thickness of each polymer film was measured using a surface profiler (Alpha-step IQ, KLA Tencor).

3. Results and discussion

The chemical structure and CV of TQTFA are shown in Fig. 1(a) and (b). The CV result reveals a reversible redox process,

allowing us to calculate the energy levels of the HOMO and LUMO according to the equation[29]

$$E_{\mathrm{HOMO/LUMO}} = [(E_{\mathrm{ox/red}} - E_{\mathrm{FC}}) + 4.8]\ \mathrm{eV}$$

On the basis of these electrochemical data, the HOMO and LUMO energy levels were −5.3 and −3.3 eV, respectively (Fig. 1(b)). Thus, TQTFA possesses intermediate energy band edges between PCBM and sufficiently large band edge offsets with P3HT and PCBM, suggesting that photoexcited excitons might be dissociated efficiently at P3HT/TQTFA, P3HT/PCBM, and TQTFA/PCBM junctions and that the carriers can be efficiently driven forward until reaching their respective electrodes (Fig. 1(c)). These phenomena were further supported by the PL emission spectra of the pristine (P3HT and TQTFA) and blended (P3HT:TQTFA, P3HT:PCBM, and TQTFA:PCBM) films (Fig. 1(d)). The PL emissions of the pristine P3HT and TQTFA films were quenched significantly upon the addition of 50 wt% TQTFA and PCBM, respectively. This highly efficient PL quenching arose as a consequence of ultra fast photoinduced charge transfer from P3HT to TQTFA and from TQTFA to PCBM. Thus, TQTFA acts as both an electron acceptor and electron donor when blended with P3HT and PCBM. Moreover, the step wise structure can accelerate the carrier transfer,[22,30,31] resulting in an increased extraction of the charge carriers. Furthermore, we expected that the wider energy differences between the LUMO energy level of the acceptor and the HOMO energy level of the donor at the P3HT/TQTFA and TQTFA/PCBM junctions would lead to elevated open-circuit voltages (V_{OC}).[32]

Compound TQTFA exhibits a wide-ranging absorption from 650 to 300 nm in its absorption spectrum (Fig. 2(a)). The absorption maximum appears at a very short wavelength (420 nm), though the absorption coefficient at this wavelength ($1.8 \times 10^5\ \mathrm{cm}^{-1}$) is as high as that of P3HT. To expand the absorption range, PC[60]BM was replaced with PC[70]BM which absorbs more light because of its less-symmetrical structure.[33,34]

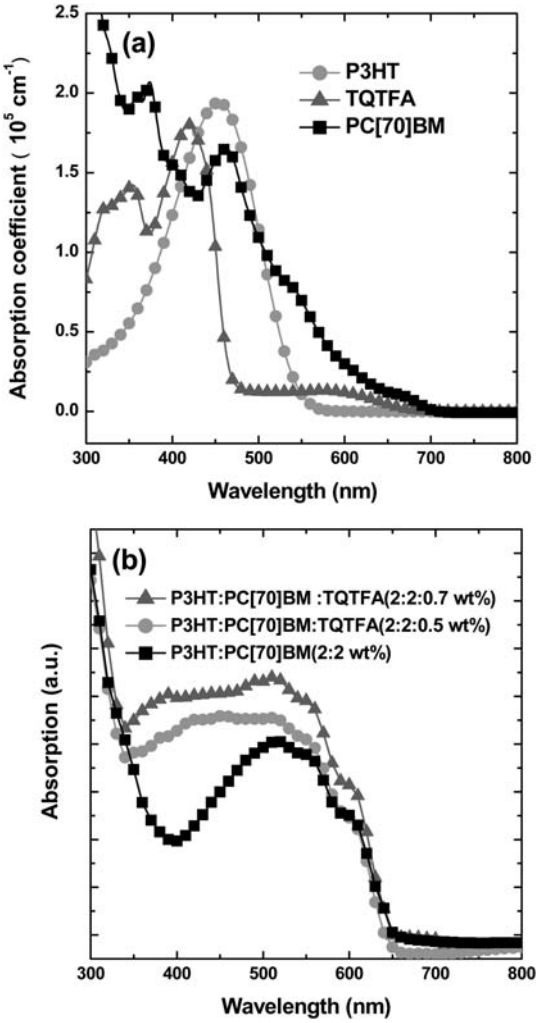

Fig. 2 (a) Extinction coefficients of TQTFA, P3HT, and PC[70]BM. (b) UV-Vis absorption spectra of blended films featuring various TQTFA ratios.

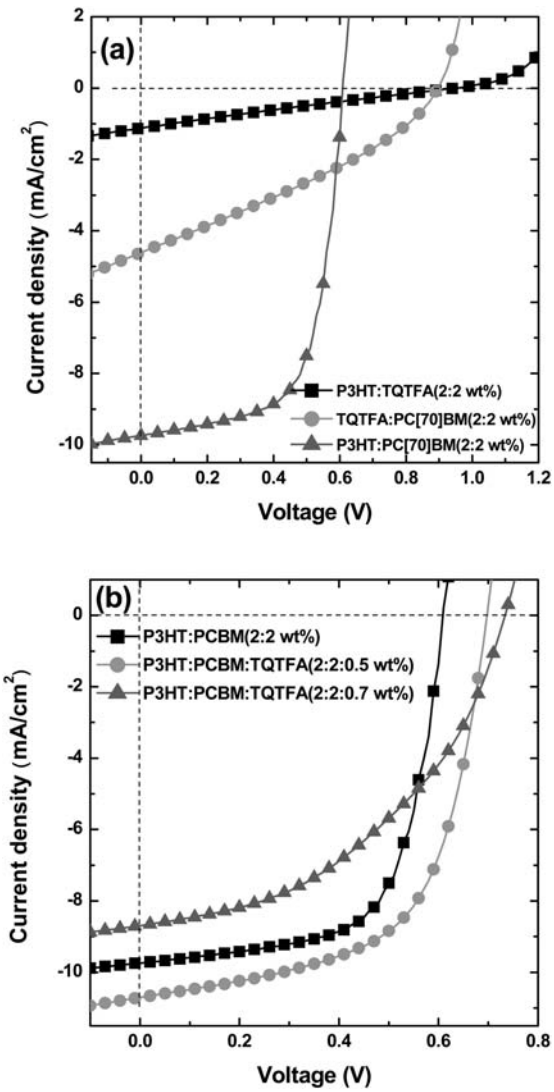

Fig. 3 *J–V* characteristics under illumination for solar cell devices incorporating (a) P3HT:TQTFA, TQTFA:PC[70]BM, and P3HT:PC[70]BM and (b) P3HT:PC[70]BM featuring various TQTFA ratios.

Fig. 2(b) reveals that the absorption between 350 and 570 nm was enhanced upon blending TQTFA with P3HT:PC[70]BM to cover almost the entire visible spectrum. We expected this broad absorption spectrum to generate a larger number of photogenerated excitons and, thus, a larger photocurrent.

Fig. 3(a) displays current density–voltage (J–V) curves for devices incorporating 1 : 1 blend ratios of TQTFA:PC[70]BM, P3HT:TQTFA, and P3HT:PC[70]BM under simulated AM 1.5 G irradiation (100 mW cm^{-2}). These layers were all fabricated *via* slow growth from 1,2-dichlorobenzene (DCB) method and subsequent annealing at 130 °C for 30 min. The P3HT:PC[70]BM device exhibited a short-circuit current (J_{SC}) of 9.74 mA cm^{-2}, a value of V_{OC} of 0.6 V, and a PCE of 3.90%. The device based on TQTFA:PC[70]BM delivered values of J_{SC} and V_{OC} of 4.60 mA cm^{-2} and 0.9 V, respectively; combined with a fill factor (FF) of 31.5%, it gave a PCE of 1.30%. The poor FFs of BHJ solar devices based on small molecules results from the high degrees of mixing between the donors and acceptors; small molecules lack the viscosity necessary for film casting, leading to extremely well mixed morphologies lacking the percolation pathways required to transport the photogenerated electrons and holes. As a result, serious charge recombination occurs, leading to low values of J_{SC} and FF. Similar results have been reported by other groups.[35–37] Furthermore, it is clear from Fig. 3(a) that the blends of P3HT and TQTFA also exhibit a photoresponse, due to the ambipolarity of TQTFA. Even though its photocurrent (1.16 mA cm^{-2}) is relatively low compared with devices based on TQTFA:PC[70]BM or P3HT:PC[70]BM, the ambipolarity of TQTFA makes it possible to prepare multi-heterojunction solar cells, thereby increasing the interface for charge separation, leading to greater photocurrents. Fig. 3(b) displays the J–V curves obtained after combining P3HT, PC[70]BM, and TQTFA at various blending ratios. Table 1 lists the measured device operating parameters J_{SC}, V_{OC}, FF and PCE with respect to the TQTFA concentration. The best devices were those cast from solutions containing 0.5 wt% TQTFA and 2 wt% of P3HT and PC[70]BM. The device cast from a solution containing 0.5 wt% TQTFA exhibited higher values of J_{SC} (10.62 mA cm^{-2}), V_{OC} (0.69 V), and PCE (4.50%) relative to those obtained for the device lacking TQTFA (9.74 mA cm^{-2}, 0.60 V, and 3.90%, respectively). These values rival those of the soluble-processed BHJ cell of a small molecule:PCBM reported recently.[38–41] For concentrations of TQTFA greater than 0.5 wt%, however, the values of J_{SC} and FF decreased upon increasing concentration; as a result, poor PCEs were obtained, even though the value of V_{OC} increased. This decrease in the values of J_{SC} and FF can be rationalized by the decreased order within the P3HT domains. Although the polymer chains of P3HT stack well during solvent annealing, its crystallinity can be destroyed if it is blended with too many small molecules, leading to an unfavorable morphology for charge transport; therefore, the devices featuring higher concentrations of TQTFA exhibited relatively low current densities and FFs (Fig. 3(b)).

Table 1 Cell performance parameters of devices incorporating various concentrations of TQTFA

P3HT:PC[70]BM:TQTFA (wt%)	J_{SC}/mA cm^{-2}	V_{OC}/V	FF (%)	PCE (%)
2 : 2 : 0	9.74	0.60	66.6	3.90
2 : 2 : 0.4	9.96	0.65	63.1	4.10
2 : 2 : 0.5	10.62	0.69	60.7	4.50
2 : 2 : 0.6	9.10	0.71	51.6	3.32
2 : 2 : 0.7	8.52	0.73	44.9	2.79

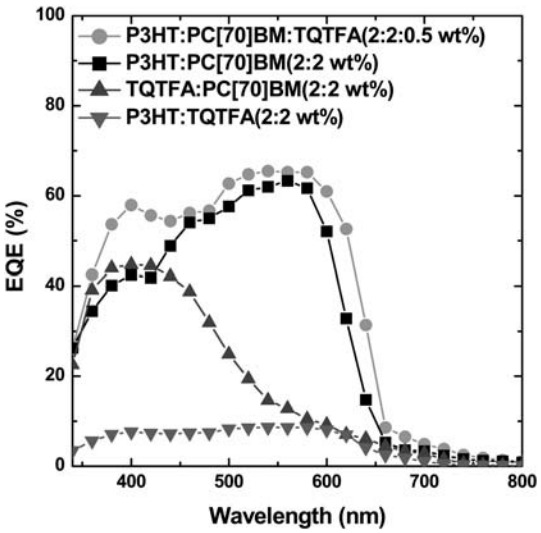

Fig. 4 EQE spectra of P3HT:PC[70]BM devices incorporating various TQTFA ratios.

EQE spectra reveal the photon–current response of devices with respect to the wavelength. Both devices based on TQTFA and PC[70]BM exhibited their maximum EQE (43.7%) at wavelength of 400 nm as illustrated in Fig. 4. This profile is similar to that of the absorption spectrum of TQTFA, indicating that the photocurrents are mainly stemmed from the absorption of the TQTFA molecules in the photoactive layer. The P3HT:TQTFA-based devices provided low EQEs under the measured wavelengths, despite the good alignment of the energy levels of P3HT and TQTFA, suggesting that the electron mobility of TQTFA is relatively poor when compared with its hole mobility. Furthermore, the EQEs of the P3HT:PC[70]BM-based device at wavelengths between 340 and 650 nm were enhanced upon blending with TQTFA, particularly in the region 340–500 nm where TQTEA had strong light absorption. Thus, incorporating a solution-processed small molecule into a polymer-based solar cell device appears to be a general method for improving the solar spectral coverage and device performance.

Fig. 5 presents tapping-mode atomic force microscopy (AFM) images (surface area: 2 × 2 μm^2) of films incorporating various blend ratios of TQTFA. The image of the P3HT/PC[70]BM blends cast from DCB in the absence of TQTFA reveals (Fig. 5(a)) coarse chain-like features stretching across the surface; we assign these features to domains of tightly stacked P3HT polymer chains. These chain-like features were less evident after blending with TQTFA. At 0.7 wt% TQTFA, the film exhibited a quite homogeneous morphology, lacking any polymer channels for charge transport; this morphology was very similar to that of the TQTFA:PC[70]BM blend film (Fig. 5(f)). Such homogeneous features lack appropriate channels for charge transport to the relative electrodes; thus, a great portion of the photogenerated electrons and holes recombined within the

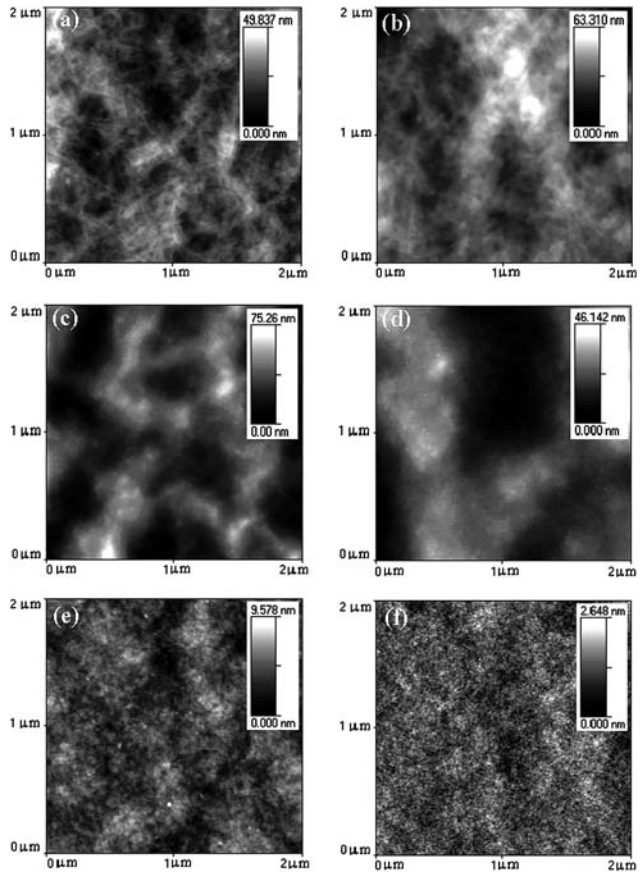

Fig. 5 AFM images of (a–e) P3HT:PC[70]BM (1 : 1) films incorporating TQTFA at (a) 0, (b) 0.4, (c) 0.5, (d) 0.6, and (e) 0.7 wt% and (f) a TQTFA:PC[70]BM (1 : 1) film. The concentration of P3HT was controlled at 2 wt%.

blends. Therefore, the solar cells incorporating high concentrations of TQTFA exhibited low values of J_{SC} and FF, as did the TQTFA:PCBM devices. Note that the blend film incorporating 0.5 wt% TQTFA possessed a rather uneven surface [root-mean-square (RMS) roughness: 12.5 nm] relative to that obtained from P3HT:PC[70]BM (RMS roughness: 9.3 nm). A rougher active surface layer can provide a rougher metal–polymer interface, which is more suitable for efficient charge collection. It should be noticed that the best device were those cast from solutions containing 0.5 wt% TQTFA and 2 wt% of P3HT and PC[70]BM. Therefore the total concentration of the two donors (P3HT and TQTFA) was controlled at 2.5 wt%. We also fabricated the BHJ devices with various ratios of P3HT and TQTFA based on the same total concentration (2.5 wt%). These results including the *J–V* characteristics and AFM images are shown in the ESI.†

4. Conclusion

In summary, we have fabricated BHJ solar cells exhibiting PCEs as high as 4.5% through solution-processing of TQTFA with P3HT and PC[70]BM to cover a wider range of the visible solar spectrum and to fine tune the energy levels to obtain higher values of J_{SC} and V_{OC}. We believe that further improvements in the performances of devices incorporating solution-processed small molecules should be possible with a more judicious choice of the energy levels of the small molecule. We also expect similar improvements for other polymer/fullerene-based systems (*e.g.*, low-band gap cells) that have already claimed efficiencies greater than 5%.

Acknowledgements

The authors are grateful to the National Science Council (NSC), Taiwan, (NSC 96-2120-M-002-016 and NSC 98-2221-E-001-002) and Academia Sinica research program on Nanoscience and Nanotechnology for financial support.

References

1 *Organic Photovoltaics: Concepts and Realization*, ed. C. J. Brabec, V. Dyakonov, J. Parisi and N. S. Sariciftci, Springer Verlag, Heidelberg, 2003.
2 J. Brabec, J. C. Hummelen and N. S. Sariciftci, *Adv. Funct. Mater.*, 2001, **11**, 15.
3 N. S. Sariciftci, L. Smilowitz, A. J. Heeger and F. Wudl, *Science*, 1992, **258**, 1474.
4 C. J. Brabec, G. Zerza, G. Cerullo, S. De Silvestri, S. Luzzati, J. C. Hummelen and N. S. Sariciftci, *Chem. Phys. Lett.*, 2001, **340**, 232.
5 W. Ma, A. Gopinathan and A. J. Heeger, *Adv. Mater.*, 2007, **19**, 3656.
6 X. Yang, J. Loos, S. C. Veenstra, W. J. H. Verhees, M. M. Wienk, J. M. Kroon, M. A. J. Michels and R. A. J. Janssen, *Nano Lett.*, 2005, **5**, 579.
7 G. Li, V. Shrotriya, Y. Yao and Y. Yang, *J. Appl. Phys.*, 2005, **98**, 043704.
8 F. Padinger, R. S. Rittberger and N. S. Sariciftci, *Adv. Funct. Mater.*, 2003, **13**, 85.
9 G. Li, V. Srotriya, J. Huang, Y. Yao, T. Moriarty, K. Emery and Y. Yang, *Nat. Mater.*, 2005, **4**, 864.
10 W. Ma, C. Yang, X. Gong, K. Lee and A. J. Heeger, *Adv. Funct. Mater.*, 2005, **15**, 1617.
11 C. J. Ko, J. K. Lin and F. C. Chen, *Adv. Mater.*, 2007, **19**, 3520.
12 L. J. A. Koster, V. D. Mihailetchi and P. W. M. Blom, *Appl. Phys. Lett.*, 2006, **88**, 093511.
13 M. C. Scharber, D. Mühlbacher, M. Koppe, P. Denk, C. Waldauf, A. J. Heeger and C. J. Brabec, *Adv. Mater.*, 2006, **18**, 789.
14 J. Peet, J. Y. Kim, N. E. Coates, W. L. Ma, D. Moses, A. J. Heeger and G. C. Bazan, *Nat. Mater.*, 2007, **6**, 497.
15 J. Hou, H. Y. Chen, S. Zhang, G. Li and Y. Yang, *J. Am. Chem. Soc.*, 2008, **130**, 16144.
16 N. Blouin, A. Michaud and M. Leclerc, *Adv. Mater.*, 2007, **19**, 2295.
17 K. G. Jespersen, F. Zhang, A. Gadisa, V. Sundstrom, A. Yartsev and O. Ingans, *Org. Electron.*, 2006, **7**, 235.
18 A. J. Moul, A. Tsami, T. W. Bünnagel, M. Forster, N. M. Kronenberg, M. Scharber, M. Koppe, M. Morana, C. J. Brabec, K. Meerholz and U. Scherf, *Chem. Mater.*, 2008, **20**, 4045.
19 F. Zhang, J. Bijleveld, E. Perzon, K. Tvingstedt, S. Barrau, O. Inganäs and M. R. Andersson, *J. Mater. Chem.*, 2008, **18**, 5468.
20 Y. Liang, Y. Wu, D. Feng, S. T. Tsai, H. J. Son, G. Li and L. Yu, *J. Am. Chem. Soc.*, 2009, **131**, 56.
21 S. Sista, Y. Yao, Y. Yang, M. L. Tang and Z. Bao, *Appl. Phys. Lett.*, 2007, **91**, 223508.
22 J. Dai, X. Jiang, H. Wang and D. Yan, *Appl. Phys. Lett.*, 2007, **91**, 253503.
23 C. Zhang, S. W. Tong, C. Jiang, E. T. Kang, D. S. H. Chan and C. Zhu, *Appl. Phys. Lett.*, 2008, **92**, 083310.
24 A. C. Morteani, A. S. Dhoot, J. S. Kim, C. Silva, N. C. Greenham, C. Murphy, E. Moons, S. Ciná, J. H. Burroughes and R. H. Friend, *Adv. Mater.*, 2003, **15**, 1708.
25 J. Huang, G. Li, E. Wu, Q. Xu and Y. Yang, *Adv. Mater.*, 2006, **18**, 114.
26 H. Kim, M. Shin and Y. Kim, *J. Phys. Chem. C*, 2009, **113**, 1620.

27 Y. Hayashi, H. Sakuragi, T. Soga, I. Alexandrou and G. A. J. Amaratunga, *Colloids Surf. A: Physicochem. Eng. Aspects*, 2008, **313**, 422.
28 M. Velusamy, J. H. Huang, Y. C. Hsu, H. H. Chou, K. C. Ho, P. L. Wu, W. H. Chang, J. T. Lin and C. W. Chu, *Org. Lett.*, 2009, **11**, 4898.
29 S. Janietz, D. D. C. Bradley, M. Grelly, C. Giebeler, M. Inbasekaran and E. P. Woo, *Appl. Phys. Lett.*, 1998, **73**, 2453.
30 T. Tominaga, K. Hayashi and N. Toshima, *Appl. Phys. Lett.*, 1997, **70**, 762.
31 B. C. Thompson and J. M. J. Frechet, *Angew. Chem., Int. Ed.*, 2008, **47**, 58.
32 J. H. Huang, C. Y. Yang, Z. Y. Ho, D. Kekuda, M. C. Wu, F. C. Chien, P. Chen, C. W. Chu and K. C. Ho, *Org. Electron.*, 200, **10**, 27.
33 M. M. Wienk, J. M. Kroon, W. J. H. Verhees, J. Knol, J. C. Hummelen, P. A. van Hal and R. A. J. Janssen, *Angew. Chem., Int. Ed.*, 2003, **42**, 3371.
34 H. Xin, X. Guo, F. S. Kim, G. Ren, M. D. Watson and S. A. Jenekhe, *J. Mater. Chem.*, 2009, **19**, 5303.
35 A. B. Tamayo, B. Walker and T. Q. Nguyen, *J. Phys. Chem. C*, 2008, **112**, 11545.
36 A. B. Tamayo, X. D. Dang, B. Walker, J. Seo, T. Kent and T. Q. Nguyen, *Appl. Phys. Lett.*, 2009, **94**, 103301.
37 J. Peet, A. B. Tamayo, X. D. Dang, J. H. Seo and T. Q. Nguyen, *Appl. Phys. Lett.*, 2008, **93**, 163306.
38 B. Waker, A. B. Tamayo, X. D. Dang, P. Zalar, J. H. Seo, A. Garcia, M. Tantiwiwat and T. Q. Nguyen, *Adv. Funct. Mater.*, 2009, **19**, 3063.
39 M. K. R. Fischer, C. Q. Ma, R. A. J. Janssen, T. Debaerdemaeker and P. Bäuerle, *J. Mater. Chem.*, 2009, **19**, 4784.
40 T. Rousseau, A. Cravino, T. Bura, G. Ulrich, R. Ziessel and J. Roncali, *J. Mater. Chem.*, 2009, **19**, 2298.
41 Z. E. Ooi, T. L. Tam, R. Y. C. Shin, Z. K. Chen, T. Kietzke, A. Sellinger, M. Baumgarten, K. Mullene and J. C. deMello, *J. Mater. Chem.*, 2008, **18**, 4619.